Journal of Cerebral Blood Flow & Metabolism (2014) 34, 753–758

www.jcbfm.com

RAPID COMMUNICATION

Diagnostic utility of amyloid PET in cerebral amyloid angiopathy-related symptomatic intracerebral hemorrhage

Jean-Claude Baron[1,2], Karim Farid[3], Eamon Dolan[4], Guillaume Turc[2], Siva T Marrapu[1], Eoin O'Brien[4], Franklin I Aigbirhio[5], Tim D Fryer[5], David K Menon[6], Elizabeth A Warburton[4] and Young T Hong[5]

By detecting β-amyloid (Aβ) in the wall of cortical arterioles, amyloid positron emission tomography (PET) imaging might help diagnose cerebral amyloid angiopathy (CAA) in patients with lobar intracerebral hemorrhage (l-ICH). No previous study has directly assessed the diagnostic value of ^{11}C-Pittsburgh compound B (PiB) PET in probable CAA-related l-ICH against healthy controls (HCs). ^{11}C-PiB-PET and magnetic resonance imaging (MRI) including T2* were obtained in 11 nondemented patients fulfilling the Boston criteria for probable CAA-related symptomatic l-ICH (sl-ICH) and 20 HCs without cognitive complaints or impairment. After optimal spatial normalization, cerebral spinal fluid (CSF)-corrected PiB distribution volume ratios (DVRs) were obtained. There was no significant difference in whole cortex or regional DVRs between CAA patients and age-matched HCs. The whole cortex DVR was above the 95% confidence limit in 4/9 HCs and 10/11 CAA patients (sensitivity = 91%, specificity = 55%). Region/frontal or occipital ratios did not have better discriminative value. Similar but less accurate results were found using visual analysis. In patients with sl-ICH, ^{11}C-PiB-PET has low specificity for CAA due to the frequent occurrence of high ^{11}C-PiB uptake in the healthy elderly reflecting incipient Alzheimer's disease (AD), which might also be present in suspected CAA. However, a negative PiB scan rules out CAA with excellent sensitivity, which has clinical implications for prognostication and selection of candidates for drug trials.

Journal of Cerebral Blood Flow & Metabolism (2014) **34,** 753–758; doi:10.1038/jcbfm.2014.43; published online 12 March 2014

Keywords: cerebral amyloid angiopathy; imaging; intracerebral hemorrhage; positron emission tomography

INTRODUCTION

Cerebral amyloid angiopathy (CAA) is an age-associated brain condition secondary to excess deposition of β-amyloid (Aβ) in the leptomeningeal and cortical arterioles.[1,2] With aging of the population, CAA has become a major cause of intracerebral hemorrhage (ICH) and is the main cause of lobar ICH (l-ICH).[1] Furthermore, CAA contributes significantly to cognitive and gait dysfunction in the elderly.[1] The clinical diagnosis of CAA-related ICH is currently based on the Boston operational criteria, which have been validated against pathologic gold standard.[3] According to these criteria, after symptomatic lobar ICH (sl-ICH), diagnosing probable CAA requires the occurrence of a second sl-ICH or the presence of at least one definite lobar microbleed (lMB) or cortical superficial siderosis (cSS) on gradient echo (GRE) magnetic resonance imaging (MRI), and no other cause identified.[3] Patients with first-ever sl-ICH who do not have lMBs or cSS therefore are diagnosed as 'possible CAA'. Given the high risk of recurrent sl-ICH which is attached with high morbidity and mortality,[1] a more precise diagnosis would be important at this early stage. In addition, novel therapeutic approaches for CAA are approaching,[4] and being able to enroll into trials CAA-related first sl-ICH at an early stage of the disease is an important objective.

^{11}C-Pittsburgh compound B (PiB) has been developed as a positron emission tomography (PET) ligand for imaging cerebral fibrillar Aβ.[5] Pittsburgh compound B binds not only to parenchymal Aβ deposits associated with Alzheimer's disease (AD) but also to cerebrovascular Aβ deposits.[5–7] Amyloid PET may therefore directly detect vascular amyloid in living patients, which would help diagnose CAA in patients with sl-ICH not fulfilling the Boston criteria for probable CAA, and also perhaps be added to the latter to increase their sensitivity and specificity. To assess the diagnostic value of ^{11}C-PiB-PET in sl-ICH, the first step is to test its sensitivity and specificity in patients diagnosed with probable CAA-related sl-ICH based on the Boston criteria as a reference.

Although a few ^{11}C-PiB-PET studies on sporadic CAA have appeared recently,[6,8–12] comparison with age-matched healthy controls (HCs) (HAMCs) is reported in three papers only.[6,10,12] In two of these reports, half of the CAA sample included nonICH presentations such as encephalopathy and seizures,[6,12] which may have different burden/distribution of Aβ deposition and hence blur the assessment of the diagnostic value of ^{11}C-PiB-PET. In the remaining article, the sample was a mix of possible and probable CAA-related sl-ICH,[10] which may affect the sensitivity of the study. Hence, no study so far has directly assessed the diagnostic value of amyloid PET imaging in probable CAA-related sl-ICH against HAMCs. The present pilot study was designed to address this issue. Given the risk of brain distortions from previous hemorrhage in CAA affecting spatial normalization of the PET and magnetic resonance images, state-of-the-art image processing was also applied here.

[1]Stroke Research Group, Department of Clinical Neurosciences, University of Cambridge, Cambridge, UK; [2]INSERM U894, Centre Hospitalier Sainte Anne, Sorbonne Paris Cité, Paris, France; [3]APHP, Hotel-Dieu Hospital, Department of Nuclear Medicine, Paris, France; [4]Stroke Unit, Addenbrooke's Hospital, Cambridge, UK; [5]Department of Clinical Neurosciences, Wolfson Brain Imaging Centre, University of Cambridge, Cambridge, UK and [6]Division of Anaesthesia, University of Cambridge, Cambridge, UK. Correspondence: Professor J-C Baron, INSERM U894, Centre de Psychiatrie et Neurosciences, Paris 75014, France.
E-mail: jean-claude.baron@inserm.fr
This study was supported by the Cambridge Comprehensive Biomedical Centre.
Received 20 December 2013; accepted 11 February 2014; published online 12 March 2014

SUBJECTS AND METHODS

Cerebral Amyloid Angiopathy Patients and Control Group

Eleven nondemented patients fulfilling current Boston criteria for probable CAA[3] (9 men, 2 women; age 70 ± 7 years; mini-mental state examination (MMSE): 26.7 ± 1.8) were recruited through the Addenbrooke's Hospital Stroke Unit or ICH clinic. Consecutive eligible patients were approached and proposed to participate in the study. As a large number of patients turned down the offer, admission records and clinic files were searched for discharged eligible patients who were then contacted by telephone. Demographic and main clinical characteristics are presented in Table 1. ^{11}C-PiB-PET was performed within 3 years of first sl-ICH. Definite lMBs were assessed at the time of PET study on GRE 3T-MRI performed as part of this protocol (see below), using the microbleed anatomical rating scale procedure.[13]

Twenty unmedicated HCs (15 men; 5 women; distribution not significantly different from the patient group; Fisher's exact test, $P = 1.00$) with no memory or cognitive complaints and with normal MMSE results (MMSE $\geqslant 29$) were also recruited through advertisements posted at the University of Third Age and hospital advert board. This sample deliberated comprised 10 HCs $\leqslant 55$ years of age (all males; NS compared with the patient group), and 10 HCs aged $\geqslant 60$ to match the age of the CAA group (5 men, 5 women; NS compared with the patient group). One HC (male) was excluded *post hoc* due to the presence of three lMBs on GRE imaging, as although lMBs are not common in healthy aged subjects, they suggest underlying CAA and are predictive of high PiB uptake.[14] The final HAMC group therefore comprised nine subjects (65 ± 5 years, NS relative to CAA; 4 men, 5 women, NS compared with CAA; MMSE range 29 to 30, $P < 0.001$).

In all subjects, white-matter hyperintense lesions were scored using the Fazekas scale[15] on fluid attenuated inversion recovery imaging (see below).

The age limit of 55 years for the young group was based on the previous studies showing no rise in amyloid tracer uptake until this age in large samples,[16–21] including ours.[22]

The Cambridgeshire Regional Ethics Committee approved this study and all participants provided signed informed consent.

Imaging Procedures: Positron Emission Tomography and Magnetic Resonance Imaging

The methodology for [^{11}C]-PiB production and PET scanning including ^{68}Ge transmission and dynamic emission scans in our center has been previously published[22] and is summarized below.

The [^{11}C]-PiB was produced at the Wolfson Brain Imaging Centre radiochemistry laboratories at high radiochemical purity ($>95\%$) and specific activity (>150 GBq/μmol) under good medicinal practice conditions.

The PET scanning was performed on a GE Advance PET scanner (General Electric, Milwaukee, WI, USA). After a ^{68}Ge/^{68}Ga transmission scan (15 minutes) for attenuation correction, ~ 550 MBq of [^{11}C]-PiB was injected as a bolus through an antecubital vein. Dynamic PET emission scanning in 3D mode was undertaken for 90 minutes after injection (58 frames: 18×5 seconds, 6×15 seconds, 10×30 seconds, 7×1 minutes, 4×2.5 minutes, and 13×5 minutes).

Magnetic Resonance Imaging

To facilitate segmentation, spatial normalization, and delineation of anatomic regions of interest (ROIs), participants also underwent a structural T1-weighted MRI scan on a 3T Siemens Tim-Trio (Siemens Medical Solutions, Erlangen, Germany), using a 3-dimensional MPRAGE scan (magnetization-prepared rapid GRE sequence; repetition time/echo time/inversion time = 2,300 milliseconds/2.98 milliseconds/900 milliseconds; flip angle, 9°; 1 average; 176 slices; 256×256 matrix size; $1 \times 1 \times 1$ mm voxel size).

The magnetic resonance protocol for this study also included standard T2* GRE and fluid attenuated inversion recovery.

Image Analysis

Generic image processing and analysis have been previously published in detail,[22] except that in the present study we implemented advanced image processing for spatial normalization (see below). Briefly, each dynamic ^{11}C-PiB-PET scan was reconstructed using the PROMIS 3D filtered backprojection algorithm,[23] with corrections applied for randoms, dead

Table 1. Patients demographics and main clinical characteristics

Patient	*Age (years)*	*M/F*	*l-ICH*[a]	*VRF*	*Main symptoms*	*Current medications*	*MMSE*	*Lobar MBs*	*Fazekas score*	*cSS*
1	58	F	L Hippocampus	D, AHT	Amnesia, dysphasia	Insulin, atorvastatine, losartan, lecardipine, paroxetine	26	>5	2	—
2	80	M	R Occ	AHT, AF	Visual field deficit	Simvastatine, candesartan, bendrofluazide, tamsulosin, gabapentin	25	1	2	Disseminated
3	78	M	L Temp	Smoking	Dysphasia, disinhibited behaviour	Haloperidol	27	3	3	Disseminated
4	75	M	R Front (L Front)	—	L hemiparesis	Lisinopril, alendronate	25	2	3	Disseminated
5	64	M	L Par, R Occ-Temp-Par	Ischemic heart disease	Poor concentration	Diltiazem, nicorandil, ezetimibe, lansoprazole	25	2	2	Disseminated
6	77	F	L Front	—	language difficulties, facial weakness	Simvastatine, alendronate, zopiclone	29	4	3	—
7	61	M	R Temp-Par	AHT, PAD, Dyslipidemia	R hemiparesis and visual field deficit	Rosuvastatin, allopurinol	30	>5	2	—
8	78	M	R Front, L Occ-Temp	D, AHT	Confusion	Perindopril, metformin, giglizide	28	>5	3	—
9	72	M	L Front (L Temp[b])	Ischemic heart disease, ex-smoker, AHT, dyslipidemia	R hemiparesis, partial complex seizures	Simvastatine, candesartan, lansoprasole, levetiracetam	26	>5	3	Disseminated
10	71	M	R Occ, R Occ, L Occ-Temp	—	visual fields disturbance	Thyroxine	28	>5	3	Focal
11	71	M	R Front, R Par	AHT	L hemiparesis, visual disturbances	Lisinopril, bendrofluazide	25	5	2	—

AF, atrial fibrillation (paroxystic); AHT, arterial hypertension; cSS, cortical superficial siderosis; D, diabetes; Disseminated, cSS affecting $\geqslant 4$ sulci; Front, frontal cortex; Focal, cSS affecting <4 sulci; l-ICH, lobar intracerebral hemorrhage; L, left; M/F, gender; VRF, vascular risk factors; PAD, peripheral arterial disease; MBs, microbleeds; MMSE, mini mental state examination; R, right; Temp, temporal cortex; Par, parietal cortex; Occ, occipital cortex. [a]Associated asymptomatic ICHs are shown in brackets. [b]ICH revealed by seizures only.

time, normalization, scatter, attenuation, and sensitivity. To reduce any deterioration due to head motion, PET images were realigned using SPM8 (www.fil.ion.ucl.ac.uk/spm/software/), which was also used to coregister the mean realigned PET image to the T1-weighted MRI and reslice all the PET images to the MRI. To allow the use of standard space ROIs and limit the risk of spatial normalization errors from stroke-induced brain distortions, the MRI, and thence the coregistered PET images, was spatially normalized to the MNI/ICBM152 T1-weighted template using the symmetric image normalization method (SyN).[24] Each normalized T1 image was segmented using SPM8 to produce gray, white, and cerebral spinal fluid (CSF) probabilistic maps, which were then smoothed with an isotropic Gaussian to approximate the PET resolution 5 cm off-axis (6.8 mm full width at half maximum).

Regions of interest were defined on these spatially normalized images[25] as the intersection between 65% and above thresholded gray-matter segments and automated anatomic labeling ROIs.[26] On the basis of previous studies in CAA, normal aging, and AD, the following cerebral gray-matter ROIs were chosen from the automated anatomic labelling atlas: calcarine, anterior cingulate, posterior cingulate, frontal, hippocampus, lateral temporal, occipital, inferior parietal, and superior parietal; in addition, a whole cortex ROI was also obtained by summing all cortical ROIs in automated anatomic labeling. To mitigate the effects of cortical atrophy from partial voluming, the smoothed CSF map was used to correct GM of each ROI time-activity curve for CSF fraction (fCSF) through division by $(1-f_{CSF})$.[27,28] Cerebral spinal fluid-corrected ROI distribution volume ratio (DVR) was estimated using the reference tissue Logan graphical method Logan[29] fitted for the 35 to 90 minutes post injection interval, with the cerebellum as the reference tissue.[30] To this end, a cerebellar cortex ROI was defined from automated anatomic labeling.

We verified that standardized uptake value (SUV) for the cerebellar ROI was not significantly different between CAA and HAMC groups ($P=0.65$).

Given that relative PiB uptake has previously been reported as highest in frontal and lowest in occipital regions in the AD-like profile[6,10] (expected to be present in a fraction of the aged HCs) as opposed to high in posterior cortical regions in CAA[6] (consistent with postmortem data[31]), we also computed the Occipital/whole cortex and Frontal/whole cortex ratios, as used before,[6,10] as well as the Occipital/Frontal ratio, expected to be high in CAA.

Visual Assessment

To mimic the clinical situation, visual assessment was also undertaken.[32] Standardized unit value images were created using the 50 to 70 minutes postinjection interval.[27] Two experienced raters (JCB and KF) independently assessed for each subject a set of 20 axial SUV images (i.e., in native space) spanning the whole brain and normalized to the cerebellar standardized uptake value with reference, displayed in pseudo-color scale (see Figure 2). This was performed blind to the subject's group, that is, HC or CAA ($N=19$ and 11 subjects, respectively). Before the visual assessment and to avoid any classification bias, brain regions showing structural damage from l-ICH on MRI in the CAA group were independently masked on the coregistered MRI by an experienced physician not participating in the study, using black squares. Similar regions were also randomly masked in an equal proportion of controls.

Each assessor classified each subject as PiB− or PiB+, looking for cortical PiB retention (classified as PiB+) or only nonspecific white-matter uptake (PiB−).[19] Interrater reproducibility was computed as Cohen's kappa. Consensus between the same two assessors was subsequently implemented for discrepant cases. The PiB+ scans were then further classified as consistent with the classic AD profile (i.e., high uptake predominantly affecting the nonmotor frontal cortex, posterior cingulate area, and posterior parieto-temporal regions, but relatively sparing the occipital cortex[6,10]) or not, denoted as 'nonAD profile'. Consensus and Cohen's kappa followed this secondary classification.

RESULTS

Study Group Characteristics

All CAA patients presented with sl-ICH (Table 1). Four patients had two sl-ICHs and one had three; in addition, two had a 'silent' l-ICH on follow-up MRI, and all had at least one lMB and significant white-matter hyperintensities (Fazekas $\geqslant 2$); cSS was present in six patients. The MRI was unremarkable in the nine HAMCs apart from mild white-matter ischemic changes (Fazekas <2 in all).

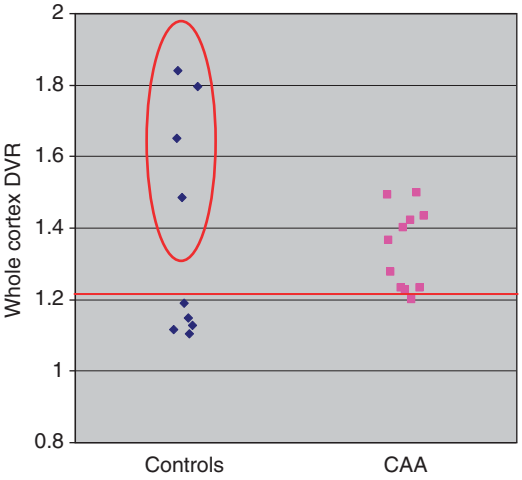

Figure 1. Whole-cortex DVR (wcDVR) values in the 9 age-matched healthy controls (HAMCs) and the 11 probable cerebral amyloid angiopathy (CAA)-related symptomatic lobar intracerebral hemorrhage (sl-ICH) patients. The horizontal line at 1.22 distribution volume ratio (DVR) denotes the cutoff for abnormally elevated whole cortex DVR (wcDVR) determined from healthy subjects $\leqslant 55$ years of age (see Subjects and Methods). The wcDVRs stand above this cutoff in 10/11 CAA patients (with the value for the last patient sitting just below it, at 1.20), as well as in 4/9 controls (circled), 3 of whom sitting above the highest wcDVR observed in the CAA patients.

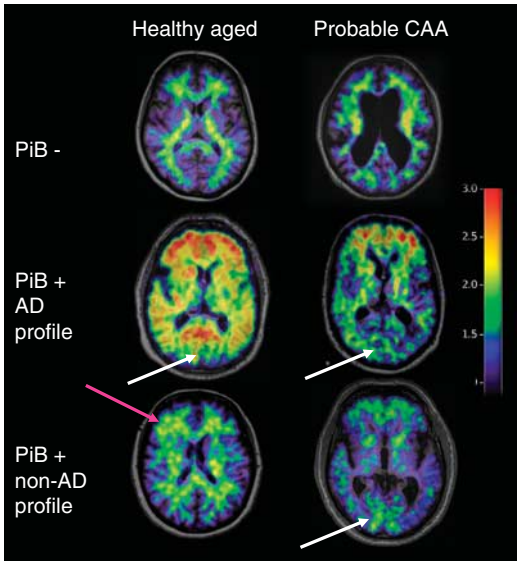

Figure 2. Representative standardized uptake value images (normalized to the subject's cerebellar value, and overlaid onto the subject's T1-weighted magnetic resonance imaging (MRI) in native space) illustrating in three subjects each from the age-matched healthy controls (HAMCs) and probable cerebral amyloid angiopathy (CAA)-related symptomatic lobar intracerebral hemorrhage (sl-ICH) groups the Pittsburgh compound B (PiB−) profile (top row), the PiB+ Alzheimer's disease (AD)-type profile (middle row) and the PiB+ non-AD profile (bottom row). The white arrows point to the posterior occipital region, which typically shows relatively low PiB uptake in the AD profile, and relatively high uptake in the PiB+ non-AD profile CAA patient shown. The pink arrow points to a right frontal cortical area with abnormal uptake in a PiB+ nonAD profile HAMC. This figure illustrates one axial slice only but the visual analysis was performed on 20 slabs per patient, covering the whole brain (see Subjects and Methods).

Pittsburgh Compound B Distribution Volume Ratio Values

There was no significant difference in either weighted-mean whole cortex DVR (wcDVR) or prespecified ROI DVRs between the CCA and HAMC groups (Table 2).

Following previously published methodology,[33] the cutoff for abnormally elevated wcDVR was derived as the upper 95% confidence interval of the young HC sample. Given the mean ($\pm$1s.d.) wcDVR in this sample was 1.108 ± 0.060 (no correlation with age, $r = 0.281$), the 95% upper confidence limit was 1.22, close to previously published values for DVR.[16,34] Relative to this cutoff, 10/11 CAA patients were PiB+, as compared with 4/9 HAMCs ($P = 0.049$, Fisher's exact test) (Figure 1). This corresponded to a sensitivity of 91%, a specificity of 55%, a positive predictive value of 71%, and a negative predictive value of 83%.

The Occipital/wc, Frontal/wc, and Occipital/Frontal ratios were not significantly different between the CAA and HAMC groups (Table 3).

Visual Analysis

Cohen's kappa for concordance of PiB+ vs. PiB− between the two assessors was 0.68 (95% confidence interval: 0.44 to 0.91) indicating substantial agreement. After consensus, 9/11 CAA patients were classified as PiB+ vs. 5/9 in the HC group (Fisher's exact test $P = 0.336$), leading to a sensitivity of 82%, a specificity of 44%, a positive predictive value of 64%, and a negative predictive value of 67%.

Subclassification of PiB+ scans as AD profile or nonAD profile demonstrated only fair interobserver reproducibility (kappa = 0.23; 95% confidence interval: −0.18 to 0.64). After consensus, 3/9 patients were classified as AD profile and 6/9 as non-AD profile in the CAA group, versus 3/5 and 2/5, respectively, in the HAMC group, a nonsignificant trend (Fisher $P = 0.58$). The sensitivity for the nonAD profile being present in PiB+ CAA patients and absent in PiB+ age-matched controls was 67%, with a specificity of 60%. Illustrative images for each group are displayed in Figure 2.

DISCUSSION

Our findings show a good sensitivity (91% and 82% for the quantitative and visual analysis, respectively) but a poor specificity (55% and 44%, respectively) of ^{11}C-PiB-PET to differentiate probable CAA from HAMCs, reflecting an almost universal PiB positivity in CAA but its frequent occurrence in healthy aged controls as well. Accordingly, there was no significant difference in PiB uptake between the two groups for any cortical region. The same applied to regional ratios expected to be sensitive to the previously reported difference in PiB pattern in CAA relative to the classic AD pattern. This is also supported by the only fair results of the visual analysis assessing the presence of a nonAD profile in PiB+ subjects. Although as will be discussed below these results are overall consistent with previous reports, this is the first study to directly assess the diagnostic value of PiB PET in probable CAA-related sl-ICH against age-matched healthy subjects.

The observed limited specificity resulted from the frequent occurrence of PiB+ healthy elderly. Indeed, based on the quantitative analysis 4/9 (44%) HAMCs were PiB positive, as compared with 10/11 CAA patients. Given the biphasic distribution in the HAMCs (Figure 1), using a more conservative wcDVR cutoff such as 1.5[35] would further strengthen, rather than weaken, this observation, since using this cutoff would result in 3/9 HAMCs versus 2/11 CAA patients being PiB+. As reviewed recently,[18,36] 20% to 40% of healthy elderly >60 years of age (and up to 50% above 80) have a significant amyloid burden on PET imaging, despite normal general cognition.[37] Our prevalence of 44% is therefore high but consistent with these ranges. It is also consistent with the CAA study of Johnson *et al*,[6] where 6/15 (40%) of their HAMCs were PiB+. Pittsburgh compound B positivity in healthy aged people is predictive of cognitive decline[35,38] and therefore likely represents asymptomatic AD. Not surprisingly, if we excluded *post hoc* the PiB+ HAMCs from our analysis, the wcDVR would become significantly higher in CAA patients (1.31 ± 0.11 vs. 1.13 ± 0.03, respectively, $P = 0.006$; similar *P*-values for all ROIs except the hippocampus). However, excluding PiB+ HCs is unwarranted merely because incipient AD might also be present in patients suspected of CAA, particularly given the frequent cooccurrence and overlapping pathophysiology of these two amyloid-related conditions.[31] Conversely, the healthy elderly may harbor incipient CAA, given the incidence of asymptomatic CAA at autopsy in healthy aged subjects is up to 50%.[31]

Importantly, despite the poor specificity of PiB for CAA, our finding that almost all CAA patients were PiB+, particularly with the quantitative analysis (91%; note that the last patient was borderline, see Figure 1), indicate that PiB imaging has high sensitivity for CAA. Accordingly, the negative predictive value was high (83%), that is, CAA can be ruled out with good confidence if ^{11}C-PiB imaging is negative. Consistent with clinical experience, the quantitative analysis was more efficient than visual inspection in our study. This finding of high sensitivity of PiB positivity for CAA is consistent with previous reports, with 6/6 (100%) and 9/12 (75%) CAA patients being PiB positive in the Johnson[6] and Ly[10] studies, respectively. However, only 2/6 patients presented with ICH in the former,[6] while in the latter 3/12 had possible CAA only. Although Gurol *et al*[12] did not formally report sensitivity, applying their reported cutoff for PiB positivity on their Figure 2 suggests

Table 3. Occipital/Whole cortex, Frontal/Whole cortex and Occipital/Frontal PiB ratios in CAA patients ($n = 11$) and healthy age-matched controls ($n = 9$) (mean $\pm$ s.d.)

	Occipital/Whole cortex	*Frontal/Whole cortex*	*Occipital/Frontal*
CAA	0.92 ± 0.06	1.04 ± 0.04	0.88 ± 0.07
Controls	0.94 ± 0.04	1.06 ± 0.03	0.88 ± 0.06

CAA, cerebral amyloid angiopathy; DVR, distribution volume ratio; PiB, Pittsburgh compound B. No comparison was statistically significant (two-sample *t*-tests).

Table 2. PiB DVR in CAA patients ($n = 11$) and healthy age-matched controls ($n = 9$) (mean $\pm$ s.d.), and *P* value for the between-groups two-sample *t*-tests

	Whole cortex	*Calcarine*	*Ant cingulum*	*Post cingulum*	*Frontal*	*Hippocampus*	*Lateral temporal*	*Occipital*	*Parietal Inf*	*Parietal Sup*
CAA	1.31 ± 0.11	1.33 ± 0.18	1.55 ± 0.23	1.38 ± 0.09	1.40 ± 0.14	1.10 ± 0.08	1.20 ± 0.13	1.23 ± 0.13	1.33 ± 0.15	1.32 ± 0.16
Controls	1.38 ± 0.29	1.36 ± 0.31	1.60 ± 0.44	1.46 ± 0.29	1.47 ± 0.32	1.14 ± 0.09	1.27 ± 0.27	1.29 ± 0.24	1.48 ± 0.34	1.46 ± 0.34
P	0.49	0.80	0.80	0.41	0.55	0.40	0.47	0.52	0.24	0.26

CAA, cerebral amyloid angiopathy; DVR, distribution volume ratio; PiB, Pittsburgh compound B.

that only around 14/42 (33%) CAA patients were PiB + ; however, only 23 patients in their sample had sl-ICH, making comparison with our results difficult.

The present pilot study enrolled a relatively small CAA sample, so confirmation of our observations is warranted. However, all our probable CAA patients had clinically well-characterized sl-ICH, and all patients and HCs underwent T2* scans, which allowed us to exclude one control who had three lMBs. As already pointed out, previous similar studies did not have such homogeneous CAA samples, which may explain their reported significant difference in wcDVR between patients and HAMCs.[6,10,12] In addition, in the Ly *et al*[10] study, 2/12 patients did not have T2* scans, and whether PiB + HCs were excluded or not remains unclear. All our patients were on at least one, and several on up to four oral medications (Table 1). Although we cannot exclude that some of these agents may have affected nonspecific PiB uptake, it has to be noted that the DVRs used to assess specific PiB uptake were derived using the cerebellum as a reference region, so in all likelihood cancelling out any such effect on nonspecific binding; furthermore, there was no significant difference in cerebellar PiB SUV between patients and controls (see Subjects and methods). Although our sample of HAMCs was also relatively small, these were strictly selected for their optimal health and lack of lMBs, cSS, or marked white-matter fluid attenuated inversion recovery hyperintensities, and it is unlikely that a larger sample would have changed the main results given the reported high incidence of PiB positivity in the aged population.[18,36] Finally, and at variance with previous studies, we used advanced image processing involving SyN for accurate spatial normalization and CSF correction of the quantitative data. This provided for optimal results though precluded the use of publicly available databases.

As already alluded to, the main issue raised by our study is the complication, intrinsic to amyloid imaging, that many aged HCs may have incipient AD and/or CAA, while probable/possible CAA patients may have incipient AD. However, a possible algorithm in suspected CAA could entail first determining PiB positivity, then assessing whether the visual PiB pattern differs from classic AD. Unfortunately, adjudicating a nonAD profile proved somewhat unrewarding in our study, as only 6/9 PiB + CAA patients had a nonAD profile after consensus, and interobserver reproducibility was only fair. However, the quantitative analysis may perform better, given previous reports that suggest significantly higher occipital/frontal ratio in CAA as compared with AD.[6,10] We tested this hypothesis in a *post hoc* analysis using a sample of seven probable AD patients[39] (mean age: 66, range 59 to 73) from our center's database, which recovered the expected difference in calcarine/frontal DVR (0.94 ± 0.10 vs. 0.86 ± 0.07 in CAA and AD groups, respectively; one-tailed $P = 0.027$). Although preliminary, these findings support the idea that amyloid imaging may be of use in diagnosing suspected CAA-related ICH according to the above two-step procedure according to a quantitative analysis. Future studies are needed to confirm this observation. Note however that 3/9 CAA patients had a definite AD profile visually (Figure 2), consistent with the recent report of a patient diagnosed as probable AD with typical AD pattern on ^{11}C-PiB-PET but pure CAA at autopsy.[40]

CONCLUSION

An early diagnosis of CAA using amyloid imaging would have important clinical impact on prognostication (i.e., risk of recurrence of sl-ICH and other complications of CAA), medical management (e.g., the issue of antiplatelet therapy in patients who have experienced an ICH) and selection of candidates for trials of disease-modifying therapies. This study found that ^{11}C-PiB-PET has low specificity for the diagnosis of CAA-related lobar ICH due to the well-established high incidence of elevated ^{11}C-PiB uptakes in the healthy elderly reflecting incipient AD, which might also be present in suspected CAA. However, our study also suggests that a negative PiB scan reliably rules out CAA, which has significant clinical implications. Further studies in possible CAA-related sl-ICH including either pathologic verification of presence of CAA or long follow-up to determine whether they convert to probable CAA will also be of considerable interest. Furthermore, using both a young HC group and an AD group as dual reference may provide an interesting approach for improved specificity. Prospective studies in large samples are warranted to confirm or refute these observations.

DISCLOSURE/CONFLICT OF INTEREST

The authors declare no conflict of interest.

ACKNOWLEDGMENTS

The authors thank the stroke physicians and research nurses for help with the recruitment of patients and healthy subjects for this study, and the WBIC cyclotron, chemistry and PET and MR radiographers for making it feasible.

REFERENCES

1 Charidimou A, Gang Q, Werring DJ. Sporadic cerebral amyloid angiopathy revisited: recent insights into pathophysiology and clinical spectrum. *J Neurol Neurosurg Psychiatry* 2012; **83**: 124–137.
2 Vinters HV. Cerebral amyloid angiopathy. A critical review. *Stroke* 1987; **18**: 311–324.
3 Linn J, Halpin A, Demaerel P, Ruhland J, Giese AD, Dichgans M *et al.* Prevalence of superficial siderosis in patients with cerebral amyloid angiopathy. *Neurology* 2010; **74**: 1346–1350.
4 Schroeter S, Khan K, Barbour R, Doan M, Chen M, Guido T *et al.* Immunotherapy reduces vascular amyloid-beta in PDAPP mice. *J Neurosci* 2008; **28**: 6787–6793.
5 Klunk WE, Engler H, Nordberg A, Wang Y, Blomqvist G, Holt DP *et al.* Imaging brain amyloid in Alzheimer's disease with Pittsburgh compound-B. *Ann Neurol* 2004; **55**: 306–319.
6 Johnson KA, Gregas M, Becker JA, Kinnecom C, Salat DH, Moran EK *et al.* Imaging of amyloid burden and distribution in cerebral amyloid angiopathy. *Ann Neurol* 2007; **62**: 229–234.
7 Greenberg SM, Grabowski T, Gurol ME, Skehan ME, Nandigam RN, Becker JA *et al.* Detection of isolated cerebrovascular beta-amyloid with Pittsburgh compound B. *Ann Neurol* 2008; **64**: 587–591.
8 Dierksen GA, Skehan ME, Khan MA, Jeng J, Nandigam RN, Becker JA *et al.* Spatial relation between microbleeds and amyloid deposits in amyloid angiopathy. *Ann Neurol* 2010; **68**: 545–548.
9 Gurol ME, Dierksen G, Betensky R, Gidicsin C, Halpin A, Becker A *et al.* Predicting sites of new hemorrhage with amyloid imaging in cerebral amyloid angiopathy. *Neurology* 2012; **79**: 320–326.
10 Ly JV, Donnan GA, Villemagne VL, Zavala JA, Ma H, O'Keefe G *et al.* ^{11}C-PiB binding is increased in patients with cerebral amyloid angiopathy-related hemorrhage. *Neurology* 2010; **74**: 487–493.
11 Ly JV, Rowe CC, Villemagne VL, Zavala JA, Ma H, O'Keefe G *et al.* Cerebral beta-amyloid detected by Pittsburgh compound B positron emission topography predisposes to recombinant tissue plasminogen activator-related hemorrhage. *Ann Neurol* 2010; **68**: 959–962.
12 Gurol ME, Viswanathan A, Gidicsin C, Hedden T, Martinez-Ramirez S, Dumas A *et al.* Cerebral amyloid angiopathy burden associated with leukoaraiosis: a positron emission tomography/magnetic resonance imaging study. *Ann Neurol* advance online publication, 13 December 2012; doi:10.1002/ana.23830 (e-pub ahead of print).
13 Gregoire SM, Chaudhary UJ, Brown MM, Yousry TA, Kallis C, Jager HR *et al.* The microbleed anatomical rating scale (MARS): reliability of a tool to map brain microbleeds. *Neurology* 2009; **73**: 1759–1766.
14 Yates PA, Sirisriro R, Villemagne VL, Farquharson S, Masters CL, Rowe CC. Cerebral microhemorrhage and brain beta-amyloid in aging and Alzheimer disease. *Neurology* 2011; **77**: 48–54.
15 Fazekas F, Chawluk JB, Alavi A, Hurtig HI, Zimmerman RA. MR signal abnormalities at 1.5 t in Alzheimer's dementia and normal aging. *AJR Am J Roentgenol* 1987; **149**: 351–356.
16 Vlassenko AG, Mintun MA, Xiong C, Sheline YI, Goate AM, Benzinger TL *et al.* Amyloid-beta plaque growth in cognitively normal adults: longitudinal [11C]Pittsburgh compound B data. *Ann Neurol* 2011; **70**: 857–861.
17 Roe CM, Fagan AM, Grant EA, Hassenstab J, Moulder KL, Maue Dreyfus D *et al.* Amyloid imaging and CSF biomarkers in predicting cognitive impairment up to 7.5 years later. *Neurology* 2013; **80**: 1784–1791.

18 Chetelat G, La Joie R, Villain N, Perrotin A, de La Sayette V, Eustache F *et al.* Amyloid imaging in cognitively normal individuals, at-risk populations and preclinical Alzheimer's disease. *Neuroimage Clin* 2013; **2**: 356–365.
19 Mintun MA, Larossa GN, Sheline YI, Dence CS, Lee SY, Mach RH *et al.* [^{11}C]PiB in a nondemented population: potential antecedent marker of Alzheimer disease. *Neurology* 2006; **67**: 446–452.
20 Rodrigue KM, Kennedy KM, Devous Sr. MD, Rieck JR, Hebrank AC, Diaz-Arrastia R *et al.* Beta-amyloid burden in healthy aging: regional distribution and cognitive consequences. *Neurology* 2012; **78**: 387–395.
21 Vandenberghe R, Van Laere K, Ivanoiu A, Salmon E, Bastin C, Triau E *et al.* 18f-flutemetamol amyloid imaging in Alzheimer disease and mild cognitive impairment: a phase 2 trial. *Ann Neurol* 2010; **68**: 319–329.
22 Landt J, D'Abrera JC, Holland AJ, Aigbirhio FI, Fryer TD, Canales R *et al.* Using positron emission tomography and carbon 11-labeled Pittsburgh compound B to image brain fibrillar beta-amyloid in adults with Down syndrome: Safety, acceptability, and feasibility. *Arch Neurol* 2011; **68**: 890–896.
23 Kinahan PE RJ. Analytic 3D image reconstruction using all detected events. *IEEE Trans Nucl Sci* 1989; **36.**
24 Avants BB, Epstein CL, Grossman M, Gee JC. Symmetric diffeomorphic image registration with cross-correlation: evaluating automated labeling of elderly and neurodegenerative brain. *Med Image Anal* 2008; **12**: 26–41.
25 Laymon CM, Rosario BL, Redfield A, Berginc M, Klunk WE, Mathis CA *et al.* Comparative evaluation of template-based region sampling for PiB Pet data analysis. *Neuroimage.* 2010; **51**: S219.
26 Tzourio-Mazoyer N, Landeau B, Papathanassiou D, Crivello F, Etard O, Delcroix N *et al.* Automated anatomical labeling of activations in SPM using a macroscopic anatomical parcellation of the MNI MRI single-subject brain. *Neuroimage* 2002; **15**: 273–289.
27 Rosario BL, Weissfeld LA, Laymon CM, Mathis CA, Klunk WE, Berginc MD *et al.* Inter-rater reliability of manual and automated region-of-interest delineation for PiB PET. *Neuroimage* 2011; **55**: 933–941.
28 Nestor PJ, Fryer TD, Smielewski P, Hodges JR. Limbic hypometabolism in Alzheimer's disease and mild cognitive impairment. *Ann Neurol* 2003; **54**: 343–351.
29 Logan J, Fowler JS, Volkow ND, Wang GJ, Ding YS, Alexoff DL. Distribution volume ratios without blood sampling from graphical analysis of PET data. *J Cereb Blood Flow Metab* 1996; **16**: 834–840.
30 Price JC, Klunk WE, Lopresti BJ, Lu X, Hoge JA, Ziolko SK *et al.* Kinetic modeling of amyloid binding in humans using PET imaging and Pittsburgh compound-B. *J Cereb Blood Flow Metab* 2005; **25**: 1528–1547.
31 Kovari E, Herrmann FR, Hof PR, Bouras C. The relationship between cerebral amyloid angiopathy and cortical microinfarcts in brain ageing and Alzheimer's disease. *Neuropathol Appl Neurobiol* 2013; **39**: 498–509.
32 Ng S, Villemagne VL, Berlangieri S, Lee ST, Cherk M, Gong SJ *et al.* Visual assessment versus quantitative assessment of 11C-PIB pet and 18F-FDG PET for detection of Alzheimer's disease. *J Nucl Med* 2007; **48**: 547–552.
33 Mormino EC, Brandel MG, Madison CM, Rabinovici GD, Marks S, Baker SL *et al.* Not quite PiB-positive, not quite PiB-negative: slight PiB elevations in elderly normal control subjects are biologically relevant. *Neuroimage* 2012; **59**: 1152–1160.
34 Sojkova J, Driscoll I, Iacono D, Zhou Y, Codispoti KE, Kraut MA *et al. In vivo* fibrillar beta-amyloid detected using [11C]PiB positron emission tomography and neuropathologic assessment in older adults. *Arch Neurol* 2011; **68**: 232–240.
35 Villemagne VL, Pike KE, Chetelat G, Ellis KA, Mulligan RS, Bourgeat P *et al.* Longitudinal assessment of Abeta and cognition in aging and Alzheimer disease. *Ann Neurol* 2011; **69**: 181–192.
36 Mathis CA, Kuller LH, Klunk WE, Snitz BE, Price JC, Weissfeld LA *et al. In vivo* assessment of amyloid-beta deposition in nondemented very elderly subjects. *Ann Neurol* 2013; **73**: 751–761.
37 Aizenstein HJ, Nebes RD, Saxton JA, Price JC, Mathis CA, Tsopelas ND *et al.* Frequent amyloid deposition without significant cognitive impairment among the elderly. *Arch Neurol* 2008; **65**: 1509–1517.
38 Resnick SM, Sojkova J, Zhou Y, An Y, Ye W, Holt DP *et al.* Longitudinal cognitive decline is associated with fibrillar amyloid-beta measured by [11C]PiB. *Neurology* 2010; **74**: 807–815.
39 McKhann G, Drachman D, Folstein M, Katzman R, Price D, Stadlan EM. Clinical diagnosis of Alzheimer's disease: report of the NINCDS-ADRDA Work Group under the auspices of Department of Health and Human Services Task Force on Alzheimer's disease. *Neurology* 1984; **34**: 939–944.
40 Ducharme S, Guiot MC, Nikelski J, Chertkow H. Does a positive Pittsburgh compound B scan in a patient with dementia equal Alzheimer disease? *JAMA Neurol* 2013; **70**: 912–914.